Hydrology and
Earth System
Sciences
Open Access
Discussions

Predicting subsurface storm flow response of a forested hillslope: the role of connected flow paths and bedrock topography

J. Wienhöfer and E. Zehe

Institute of Water Resources and River Basin Management, Karlsruhe Institute of Technology, Karlsruhe, Germany

Correspondence to: J. Wienhöfer (jan.wienhoefer@kit.edu)

Discussion Paper | Discussion Paper | Discussion Paper | Discussion Paper

HESSD

10, 6473–6514, 2013

Predicting subsurface storm flow response

J. Wienhöfer and E. Zehe

Title Page

Abstract | Introduction

Conclusions | References

Tables | Figures

|◄ | ►|

◄ | ►

Back | Close

Full Screen / Esc

Printer-friendly Version

Interactive Discussion

J. Wienhöfer and E. Zehe

Title Page

Abstract | Introduction

Conclusions | References

Tables | Figures

◀◀ | ▶▶

◀ | ▶

Back | Close

Full Screen / Esc

Printer-friendly Version

Interactive Discussion

Abstract

Rapid flow processes in connected preferential flow paths are widely accepted to play a key role for rainfall-runoff response at the hillslope scale, but a quantitative description of these processes is still a major challenge in hydrological research. This paper investi-
gates the approach of incorporating preferential flow paths explicitly in a process-based model for modelling water flows and solute transport at a steep forested hillslope. We conceptualise preferential flow paths as spatially explicit structures with high conductivity and low retention capacity, and evaluate simulations with different combinations of vertical and lateral flow paths against measured discharge and tracer breakthrough.
Out of 122 tested realisations, five setups fulfilled our selection criteria for the water flow simulation. These setups successfully simulated infiltration, vertical and lateral subsurface flow in structures, and allowed predicting the magnitude, dynamics and water balance of the hydrological response of the hillslope during subsequent periods of steady-state sprinkling on selected plots and intermittent rainfall on the entire hillslope area. The solute transport simulations with these setups matched spread and shape of the observed breakthrough curve well, indicating that macrodispersion induced by preferential flow was captured well by the topology of the preferential flow network. The model, however, could not match the very fast breakthrough times observed in the tracer experiment. This can readily be attributed to the simplified representation of the spatial dimensions of the implemented distinctive structures in the 2-D cross-section, which led to an underestimation of effective transport velocities in comparison to the correctly modelled flux densities.
The configurations of successful model setups suggest that preferential flow bound to connected vertical and lateral flow paths is a first-order control on the hydrology of the study hillslope, whereas spatial variability of soil depth is secondary. Virtual experiments for investigating hillslope controls on subsurface processes should thus explicitly consider distinctive flow paths as a potential determinant.

1   Introduction

Understanding how the internal architecture of hillslopes controls subsurface flow and transport processes and predicting this interplay with models "that work for the right reasons" are still unsolved problems in hillslope hydrology, but also of considerable importance for hydrological predictions at larger scales.

Structures and patterns play a key role in the organisation of hydrological processes across scales (Vogel and Roth, 2003; Schulz et al., 2006; McDonnell et al., 2007). In the context of soil hydrology it is well known that structural features like pipes and macropores generated by plant roots and animals, or soil cracks from desiccation, offer much less resistance to gravity-driven flows than the surrounding soil matrix, and hence allow rapid flow and transport rates, which had led to the term "preferential flow" (Beven and Germann, 1982; Flury et al., 1994). Together with bedrock and soil matrix, these preferential flow pathways determine the subsurface flow characteristics of a hillslope (Peters et al., 1995; Buttle and McDonald, 2002; Uchida et al., 2005; Kienzler and Naef, 2008). Connected networks of preferential flow paths facilitate rapid vertical and lateral transport of water and solutes in the subsurface over considerable distances (Sidle et al., 2001; Anderson et al., 2009a; Wienhöfer et al., 2009a; Baram et al., 2012). This occurrence of preferential flow is bound to the existence of distinctive void structures (Sanders et al., 2012), although the actual preferential flow path may involve the soil matrix around active macropores (Lamy et al., 2009). These rapid flow processes pertain to the runoff mechanism termed subsurface storm flow (Weiler et al., 2006), which dominate the processes involved in runoff generation in response to heavy rainfall at the scale of hillslopes and small catchments, especially at steep hillslopes in temperate humid climates (Bonell, 1993; Uchida et al., 1999; Weiler and McDonnell, 2007; Zehe and Sivapalan, 2009; Jones, 2010). Vertical preferential flow is furthermore an important determinant for leaching and fates of agrochemicals through the vadose zone and related soil and groundwater pollution (Flury et al., 1995; Zehe and Flühler, 2001; Clothier et al., 2008). Fast lateral flows have also been related to slope stability

Predicting subsurface storm flow response

J. Wienhöfer and E. Zehe

Title Page

| Abstract | Introduction |

| Conclusions | References |

| Tables | Figures |

Back | Close

Full Screen / Esc

Printer-friendly Version

Interactive Discussion

(Uchida et al., 2001; Lindenmaier et al., 2005; Hencher, 2010; Wienhöfer et al., 2011; Krzeminska et al., 2012). Consequently, it is highly relevant to incorporate preferential flow processes in models for predicting flow and transport through the vadose zone.

1.1 Modelling of preferential flow processes

Deterministic, spatially explicit models are widely used for simulation of water and solute transport in soils from the core to the field scale. The representation of macropores, i.e. pores with equivalent diameters of more than 1 mm or even much larger structures (Beven and Germann, 1982; Luxmoore et al., 1990), and their hydraulic effects has been the subject of numerous studies, and a variety of modelling concepts have been proposed. These are covered in detail by a couple of excellent review articles (Šimůnek et al., 2003; Jarvis, 2007; Gerke, 2006; Köhne et al., 2009). The model concepts to account for preferential flow range from alterations of the classical Darcy–Richards model by modification of the unsaturated hydraulic conductivity functions (Durner, 1994; Zehe et al., 2001; Kelln et al., 2009), to dual-domain models that conceptually split the soil into a matrix and a preferential flow domain (Gerke and Vangenuchten, 1993; Tsutsumi et al., 2005; Stadler et al., 2012).

Generally, spatially explicit approaches are based on the concept of a representative elementary volume (REV) as the basic element of the model. The parameterisation of the REV reflects a representative spatial average of the actual structure of the pore-space, which has a length scale typically much smaller than the spatial discretisation of the model. In the same way, the spatial configuration of macropores is represented implicitly in most models, even when flow processes in micropores and macropores are conceptually separated in different domains. Some studies, however, have incorporated preferential flow structures explicitly as discrete fine-scale elements within a spatially explicit model in order to geometrically separate preferential flow paths from the micro-structure of the soil. This strategy has been adopted in numerical experiments to investigate the role of soil pipes for subsurface stormflow (Nieber and Warner, 1991), the role of earthworm burrows for dissipation of free energy (Zehe et al., 2010a), and

the effect of disconnected macropores on preferential flow (Nieber and Sidle, 2010). Moreover, the approach has been successfully tested against experimental data; for example for modelling lab-scale experiments with soil cores containing artificial vertical macropores (Allaire et al., 2002a,b; Castiglione et al., 2003; Lamy et al., 2009) and sloping soil blocks containing artificial lateral pipes (Kosugi et al., 2004; Tsutsumi et al., 2005).

Although an explicit consideration of macro-structures is conceptually appealing and instrumental in investigating hydrological processes across scales (Vogel and Roth, 2003), the approach has been rarely tested with field experiments, because detailed information on subsurface flow paths is typically not available at the majority of study sites. It has to be acquired in the field by marking flow paths with dye or other substances and carefully excavating the soil (Noguchi et al., 1999; Anderson et al., 2009b; Abou Najm et al., 2010). These methods are destructive and require tremendous efforts when applied above the profile scale. The application of non-invasive geophysical imaging techniques is promising (Samouelian et al., 2003; Tabbagh et al., 2007), but these are currently not able to resolve preferential flow paths in the field (Moysey and Liu, 2012; Greve et al., 2010; Bievre et al., 2012). It has been shown that random placement of structures (Weiler and McDonnell, 2007) and genetic modelling of structure formation (Vogel et al., 2006) are promising ways of representing structures in process-based models when direct information is not available. This route has been recently followed by Klaus and Zehe (2010, 2011) for modelling a field-scale transport experiment at a tile-drained site. They tested different realisations of stochastically generated structures for representing vertical earthworm burrows in a 2-D model. Several of these realisations performed equally well in simulating the flow response (Klaus and Zehe, 2010), and tracer transport was acceptably reproduced by a subset of these behavioural model architectures (Klaus and Zehe, 2011).

Title Page

Abstract Introduction

Conclusions References

Tables Figures

◄ ►|

◄ ►

Back Close

Full Screen / Esc

Printer-friendly Version

Interactive Discussion

J. Wienhöfer and E. Zehe

1.2   Outline and objectives of the paper

In this paper we adopt and refine the modelling concept of Klaus and Zehe (2010, 2011), and examine its applicability for modelling a hillslope-scale sprinkling and tracer experiment at a natural forested site (Wienhöfer et al., 2009a), where plot-scale observations of prominent vertical and lateral macropores have been linked to very fast hillslope-scale transport of water and solutes. We conceptualise these flow structures as elements with high hydraulic conductivity and low retention capability at a fine spatial resolution, and implement different combinations within the Richards-based CATFLOW model to simulate both the hydraulic response of the hillslope to steady-state sprinkling and transient natural rainfall, as well as tracer transport.

The general objective of this study is to further explore the approach of explicit representation of structures for physically-based modelling at the hillslope scale. The specific objectives are to model the hillslope-scale tracer and sprinkling experiments and to investigate the hydrological functioning of preferential flow paths at the study site. For these purposes, it is essential both to compare the results of the simulations with measured data, and to critically examine the underlying perceptual, conceptual and numerical models and the relations between each other. Before these are discussed in detail, we briefly introduce the study site and relevant aspects of the field experiment, and provide information on the CATFLOW model and how we used it.

2   Methods

2.1   Study site and relevant field observations

The focus of this paper is on hillslope-scale modelling of rapid flow and transport processes observed at a natural forested site (Fig. 1). The hillslope we seek to model pertains to the study area *Heumöser* in the Vorarlberg Alps (Austria), for which a short overview is given below; further information is provided by Lindenmaier et al. (2005),

Lindenmaier (2008) and Wienhöfer et al. (2009a, 2011). The *Heumöser* belongs to the headwater catchments of the Ebniterach, which is the main tributary of the river Dornbirnerach that drains into the Lake Constance parallel to the Rhine, and is situated 10 km south-east of the city of Dornbirn and 0.5 km south of the village of Ebnit (47°21′0.2″ N, 9°44′46.62″ E). The elevation ranges from 940 to 1360 m, and the site is marked by temperate humid climate with average annual precipitation sums of about 2100 mm. The major part of precipitation (1300 mm) is rainfall during the summer months (April–September), with average monthly rainfall depths between 160 and 250 mm and intensities of up to 12 mm in 10 min. Mean annual temperature is around 7 °C and annual evapotranspiration accumulates to 500–600 mm.

The hillslope is a small subcatchment of 1232 m^2 on the steep side slopes in the south-western part of *Heumöser*. The vegetation there comprises of loose stands of common spruce (*Picea abies*) and sycamore (*Acer pseudoplatanus*), and herbaceous understorey. Slope angles vary between 18 and 54° (median: 30°). The hillslope is the source area of a perennial spring, and was considered a key area for understanding subsurface flow processes that possibly influence slope movements in the central parts (Lindenmaier, 2008; Wienhöfer et al., 2011). This motivated a couple of field investigations to collect information on subsurface characteristics with the help of soil sampling, lab and in-situ measurements, and combined sprinkling and tracer experiments. The findings relevant to our modelling study are summarised in the following; some of these have been published in further detail before (Wienhöfer et al., 2009a,b).

2.1.1 Soils and their hydraulic properties

Soils are siltic and vertic Cambisols in the midslope, and stagnic and gleyic Cambisols and Gleysols at the hillslope toe. Porosities in the topsoil (0–10 cm) are between 0.48 and 0.73, with a median of 0.58. Bulk densities are low and range from 0.5 to 1.1 g cm^{-1}, with a median of 0.63 g cm^{-1}. Soil texture is sandy loam. Below a depth of 10 cm soil textures are significantly finer, classified as silt loam and silty clay loam. Soil depths were measured with a manual auger at 63 locations, and were found to

vary between 0.12 m to > 1.10 m (median value 0.70 m; at 8 locations bedrock was not reach at 1.10 m depth). There was no clear trend in variation of soil depths with measuring position along the slope line.

The bulk hydraulic conductivity of the soil was measured in situ under field-saturated conditions with a compact constant head permeameter, and was found to decrease from values around 2×10^{-5} m s^{-1} at 12.5–25.0 cm depth to values in the range of 10^{-6} to 10^{-7} m s^{-1} at 30.0–100.0 cm depth. The measured values include the hydraulic effect of macropores, which becomes apparent by the fact that the device's maximum measurable outflow rate of ca. 1×10^{-4} m s^{-1} (Sobieraj et al., 2004) has been exceeded at one-fifth of the measurement locations ($n = 41$). The bulk values measured in the field have been corroborated by laboratory constant head permeability tests on large undisturbed soil columns from the hillslope. Additionally, multistep outflow experiments have been performed on similar soil columns under unsaturated conditions. These allowed determination of soil hydraulic parameters of the soil matrix; for example, average saturated hydraulic conductivity of the soil matrix between 0.36 to 0.72 m depth was determined to be 1.77×10^{-7} m s^{-1} (K. Germer, personal communication, 2011).

The relevance of preferential flow via macropores at this hillslope was further evidenced by plot-scale dye staining experiments. Dye infiltration was spatially uniform in the upper (0–15 cm) organic-rich soil layer; in lower horizons flows converged vertically into desiccation cracks with apertures up to 1.5 cm and root pipes with diameters of up to 4.8 cm. Besides vertical percolation, also lateral flow was observed in cracks, horizontal root pipes, and along the bedrock surface. Prominent pipes were also observed during excavation of soil cores in the study area.

2.1.2 Tracer and rainfall simulation experiments

Tracer experiments at the site showed that these distinct structures form a preferential flow network which generated fast subsurface transport at the hillslope scale. These experiments involved rainfall simulation with sprinklers at four plots located along the slope line, tracer application at three of these plots, and measurements of tracer

concentrations and discharge at two locations at the hillslope toe (Wienhöfer et al., 2009a). We focus in this paper on the hillslope tracer experiment conducted in 2007 and parts of the measurements taken at the location "cut-bank", where a hiking trail cuts the hillslope and water was observed seeping out from the subsurface. Two periods of sprinkling with $12\,mm\,h^{-1}$ on a total area of $106\,m^2$ produced a nearly steady-state discharge of 0.08–$0.10\,L\,s^{-1}$; surface runoff was not observed. Natural rainfall with a total of $94\,mm$ occurred during the $48\,h$ after the rainfall simulations and produced much higher discharges. The fluorescent dye tracer uranine was applied during the first sprinkling period under steady discharge conditions at the sprinkler plot $28.7\,m$ uphill from the cut-bank (experiment "Uranine 1" in Wienhöfer et al., 2009a). Tracer breakthrough was fast, as generally in all of the tracer tests at this site; in this case, breakthrough and peak velocities were $1.04 \times 10^{-2}\,m\,s^{-1}$ and $3.95 \times 10^{-3}\,m\,s^{-1}$, respectively.

The smooth breakthrough curve was analysed by the method of moments and fitting to a one-dimensional convection-dispersion model. The parameters obtained from the moments of the travel time probability density function resulted in low Peclét numbers (3.3 for experiment "Uranine 1"). This illustrates that flow and transport after a distance of almost $30\,m$ was still in the "near field" and far away from being well mixed. Yet, this approach does not allow further conclusions on the underlying structures and processes. This analysis indicated, however, that the tracer uranine was not retarded compared to conservative salt tracers, and that all measurements at the location cut-bank under steady-state conditions sampled the same flow field. Another important aspect was the low recovery of the tracer; only $2.93\,\%$ of the total applied tracer mass was contained in the breakthrough curve of the first stage of the experiment considered in this paper. A considerable loss of tracer was observed in column experiments with undisturbed soil material, probably due to irreversible sorption in the topsoil. This finding justified a correction of the recovery rate to account for the mobile fraction of the tracer only, which then resulted in a recovery rate of $13.32\,\%$ for the experiment "Uranine 1".

Full Screen / Esc

Printer-friendly Version

Interactive Discussion

2.2 Modelling approach

The objective of the paper is to test whether an explicit consideration of discrete preferential flow structures allows successful reproduction and prediction of water flow and solute transport at the hillslope described above. To this end we employ the numerical
5 modelling software CATFLOW, and test different spatial model setups that are consistent with the available field observations.

2.2.1 Numerical model

CATFLOW is a physically-based model for simulation of water and solute transport at the hillslope and catchment scale (Maurer, 1997; Zehe and Flühler, 2001), which
10 has been applied successfully in a number of studies (Zehe and Blöschl, 2004; Zehe et al., 2005, 2010a,b; Graeff et al., 2009; Klaus and Zehe, 2010, 2011). The basic modelling domain in CATFLOW is a hillslope, which is represented in the model as 2-D cross-section along the line of steepest descent. The third dimension perpendicular to the slope line is only represented by the width of the slope for each node; other-
15 wise, uniformity is assumed. The 2-D profile is discretized by curvilinear orthogonal coordinates, and soil water dynamic is described by the Richards equation in its potential form, which is solved numerically by an implicit mass conservative Picard iteration scheme (Celia et al., 1990). The simulation time step is dynamically adjusted to achieve optimal convergence of the iteration scheme. Soil hydraulic functions can be described
20 using several parameterisations; in the simulations presented here the parameterisation after van Genuchten (1980) and Mualem (1976) has been employed. Rainfall is partitioned into throughfall and interception storage, from which water may evaporate. Evaporation and transpiration are simulated based on the Penman–Monteith equation, taking into account the annual cycles of plant morphological and plant physiological
25 parameters, albedo as a function of soil moisture and the impact of local topography on wind speed and radiation. In the case of infiltration excess or saturation excess, surface runoff is routed along the slope line using the diffusion wave approximation of

the 1-D Saint–Venant equation, which is solved numerically with an explicit upstream finite difference scheme.

Solute transport is simulated in CATFLOW with a particle tracking scheme based on a Random Walk approach. The deterministic part of a particle step is determined by the current seepage velocities in each principal direction of the curvilinear grid using a backward two level Runge–Kutta scheme (Roth and Hammel, 1996). The random part of the particle step involves the time step, a dispersion coefficient and a uniformly distributed random number in the interval $[-1, 1]$. In the original version of the CATFLOW code, the seepage velocities acting on a particle at its current position are interpolated from the surrounding simulation nodes, ensuring a continuous velocity field. For the present attempt to model flow and transport in distinct structures, which are represented by individual simulation nodes, we seek to preserve the sharp contrasts in seepage velocities between adjacent nodes, for example macropores and soil matrix. We have therefore slightly modified the CATFLOW code; in the version used in this study, the seepage velocities for the particle step are not interpolated between nodes, but the seepage velocity of the actual simulation cell is used. Solute transport via surface runoff is not implemented in either version of CATFLOW.

2.2.2 Perceptual and conceptual model of discrete preferential flow paths at the study site

The field observations summarized above point out that prominent macropores in form of pipes and cracks constitute a connected network of vertical and lateral preferential flow paths within the fine-textured soils at the hillslope. A conductive top soil layer of low density and the soil-bedrock interface were additionally observed to influence infiltration and subsurface flow. The perception on the presence and characteristics of these different features stemmed from direct observations at separate spots. We did not have direct information on their spatial configuration over the extent of the hillslope. Nevertheless, with the observed fast breakthrough of the tracers in the experiments it is straightforward to hypothesize that the different structures form a connectedpreferential

flow network which spans the entire hillslope. This implies that vertical and lateral pathways are present at many, if not all segments of the hillslope, and that these structures directly or indirectly interconnect with each other. This is similar to the perceptual model of subsurface flow paths in a forested slope segment presented by Noguchi et al. (1999) and Sidle et al. (2001).

2.2.3 Model setup and structure generation

For the implementation of the perceptual model in CATFLOW, we basically adopted the concept of Klaus and Zehe (2010) of representing preferential flow paths explicitly as an artificial porous medium with low hydraulic resistivity, i.e., high hydraulic conductivity and low retention properties. This approach has also been followed by other studies (Nieber and Warner, 1991; Castiglione et al., 2003; Lamy et al., 2009; Nieber and Sidle, 2010).

The starting point for setting up the models was a simulation grid in fine spatial resolution, which is necessary to specify the preferential flow structures explicitly. We chose a grid size of 0.05 m × 0.05 m for the initial discretisation of a cross-section with a horizontal length of 65.0 m and a thickness of 1.8 m. The surface topography, and thus the geometry of the upper boundary, was taken from a laser-scan digital elevation model with 1 m resolution. The geometry of the lower boundary was defined by shifting the upper boundary by the thickness of 1.8 m perpendicular to the start of the slope line (Fig. 2). This basic configuration was then combined with implementations of structures which had been observed facilitating preferential flow at the study site. The grid nodes corresponding to the respective structures were assigned material parameters modelling a low flow resistivity as detailed below.

The loose and litter-rich top soil layer was assigned at the topmost row of the simulation grid (hereafter referred to as "litter layer"). As the outer nodes of the simulation grid are considered with only half of the discretisation distance, the thickness of this layer was 0.025 m. The cracks and pipes within the soil matrix were conceptualised as vertical and lateral pathways in the two-dimensional cross-section. As the

Predicting subsurface storm flow response

J. Wienhöfer and E. Zehe

Title Page

Abstract	Introduction
Conclusions	References
Tables	Figures

◀◀   ▶▶

◀   ▶

Back   Close

Full Screen / Esc

Printer-friendly Version

Interactive Discussion

exact configuration of these structures remained unknown, they were generated us-
ing random components. We used a Poisson process to allocate the starting points
of the vertical structures sequentially along the soil surface, and specified three differ-
ent minimum distances (1 m, 2 m, and 4 m) between two neighbouring starting points.
The variation of this minimum distance effectively determined density and thus the to-
tal number of vertical structures. While extending the structures stepwise into depth,
a lateral step was allowed with a probability of 10 % in order to make the structures
slightly tortuous. The final depth of the structures was drawn from a normal distribution
(mean 0.9 m, standard deviation 0.05 m), with the pathways ending in the lateral struc-
ture when this was present, and not extending into bedrock in either case. A lateral
preferential pathway within the soil matrix was generated in a similar manner, starting
at the right boundary at a depth of 0.45 m, which corresponds to one-quarter of the
total thickness of the modelled profile. This structure (hereafter referred to as "lateral
pathway") was extended stepwise towards the left boundary, allowing for upward and
downward steps with a probability of 3 % each while keeping a minimum separation of
2 m between two bendings. To ensure comparability between different model setups,
a constant random seed was used for generating the stochastic components. To deter-
mine the grid nodes with bedrock material, the measured soil depths were interpolated
using ordinary kriging. In the simulations we used either a variable bedrock topography
obtained by mapping the line of steepest descent of the interpolated bedrock topogra-
phy onto the 2-D cross-section, or a constant soil depth of 0.85 m, corresponding to the
mean soil depth of the variable topography. A soil-bedrock interface was implemented
as a continuous layer framing the resulting bedrock topography (Fig. 2).

Systematic combination of the different variants of the five structural features de-
scribed above led to 64 different model setups, supplemented by a setup without any
of these features. Further setups were obtained by modification of selected realiza-
tions, namely widening the lateral pathways, increasing the number of vertical path-
ways, limiting the vertical structures to the upper or the lower half of the hillslope, and
varying the soil hydraulic conductivities for the structures (Table 1). For the purpose

of comparison, homogeneous setups with the soil parameters of the preferential pathways and the litter layer (Table 2) were built. In total, 122 different model setups were simulated, plus a number of preliminary test runs that were performed beforehand and helped in defining the final modelling procedure.

After combining the various structure realisations with the base geometry, the initial discretisation was thinned out in model regions without preferential pathways in order to reduce the total number of nodes and thus the computational cost of the simulations. The fine grid size of 0.05 m was retained in the horizontal dimension for the vertical structures including the adjacent matrix nodes; in the vertical dimension it was kept at 0.05 m for the topmost three rows, for the lateral pathway and the soil-bedrock interface and the rows directly adjacent to these structures as well as for the endings of the vertical structures. For all other nodes, the spacing was widened up to a maximum of 0.5 m in the horizontal and 0.15 m in the vertical dimension.

All pre- and post-processing steps were carried out with help of the R environment (R Development Core Team, 2011).

2.2.4 Parameterisation of soil and structures

The hydraulic properties of the different materials were modelled with a van Genuchten–Mualem parameterisation. For parameterisation of the soil matrix we used a parameter set that had been determined by multistep-outflow experiments on large (0.108 m^3) undisturbed soil columns from the centre of the hillslope (K. Germer, University of Stuttgart; unpublished data). These parameters had been determined under unsaturated conditions to exclude hydraulic effects of macropores to the greatest possible extent. The parameters for the macroporous structures were chosen to represent a material with low flow resistivity and water retention following Castiglione (2003) and Klaus and Zehe (2010). The litter layer was likewise parameterised as a highly conductive medium with high porosity, whereas a low hydraulic conductivity and a low porosity were assigned to the bedrock material.

The transport parameters were chosen to model an ideal and nonreactive tracer. The isotropic effective dispersion coefficients of the different materials were chosen to include the effect of molecular diffusion and hydromechanical microdispersion due to sub-scale structures. Hydromechanical macrodispersion was not to be considered in the dispersion parameters, as macrostructures were modelled explicitly in this study, and thus rather low dispersion coefficients were selected. The highest dispersion coefficient was chosen for the soil matrix, whereas for the value for the bedrock was only twice as high as the diffusion coefficient in water, which for uranine is of the order of 5×10^{-10} m^2 s^{-1} (Casalini et al., 2011). All parameter values are given in Table 2.

2.2.5 Sequence of simulations and boundary conditions

The various model setups were subjected to a succession of simulations, namely two one-week spin-up runs, the sprinkling phase of the experiment, during which the input was effected at the four experimental plots, and the natural rainfall phase, which occurred after the sprinkling experiment and during which the rainfall forcing comprised the entire hillslope. The final states of the preceding run served as initial condition for the following run. The first spin-up run was started from field-saturated conditions, and was then rerun starting from the simulated final conditions. The boundary conditions at the surface were determined using meteorological data from the climate station at *Heumöser*, the known sprinkling rate during the experiment and rainfall data from a tipping bucket rain gauge located next to the hillslope. A free outflow boundary condition and a gravitational flow boundary condition were prescribed at the right and the lower boundary, respectively.

A constant width of 1.75 m was assigned for the first two runs, corresponding to the width of the experimental plots, which results in a surface area of 145.20 m^2. The third run was performed with variable widths along the slope line, representing the shape of the subcatchment with a total surface area of 1231.58 m^2 (Fig. 1). To determine the initial conditions for the total area run from the final state of the plot-scale runs, we calculated a weighted average of the water contents and solute concentrations of the

areas affected and not affected by sprinkling, respectively. This was done individually for each soil type.

2.2.6 Model evaluation

To evaluate the simulation results, the observations were compared with total simu-lated runoff, calculated as the sum of surface runoff and water fluxes across the right boundary. Runs were deemed acceptable when they showed a NSE greater than 0.75, and matched the observed water balance by 10 %. As no significant amount of surface runoff had been observed during the sprinkling experiments, model setups with a sur-face runoff ratio greater than 10 % of the total runoff during the sprinkling phase were discarded. Solute breakthrough curves were taken from the simulated solute transport over the right boundary of the model domain. For comparison of simulated and ob-served solute breakthrough, we calculated the times to first breakthrough and to the peak, and the maximum cross-correlation of the breakthrough curves.

3 Results

3.1 Simulated and observed hillslope runoff

Of the 65 systematically combined model setups, 22 runs produced acceptable matches of simulated and observed hydrographs with a NSE higher than 0.75 (maxi-mum NSE 0.86), and 38 model setups matched the observed water balance within an error of ±10 % (minimum error 1 %). A surface runoff ratio of less than 10 % of total runoff during the sprinkling phase was found for 24 model setups, while in 27 simu-lations surface runoff constituted more than 90 % of total outflow during the sprinkling phase.

Five of the model setups fulfilled all three criteria. The corresponding hydrographs are displayed in Fig. 3a–e, and the details of the model setups are summarised in Table 3. It is noticeable that all of these five setups involved the presence of vertical

structures and constant depth to bedrock. In each setup at least one lateral pathway was present, either the lateral structure or the soil-bedrock interface, or both. A loose top-soil layer (litter layer) was not present in two of the five runs, and these also were setups with a higher number of vertical structures. In a reference setup without any structures, the entire hillslope outflow occurred as surface runoff (Fig. 3f). This setup is thus to be rejected, because no significant amount of surface runoff had been observed in the field. Additionally, the NSE for this setup is rather low (NSE = 0.31), as the simulated response during the rainfall phase is rising and falling much more abruptly than observed, although the hydrograph during the sprinkling phase is matched well. Similar setups without structures, but with parameterising the entire soil domain above bedrock with the material parameters of the litter layer and the preferential pathways (Table 2), respectively, yielded only right boundary flux and not any surface runoff. The hydrographs resulting from these uniform parameterisations were strongly damped and delayed compared to the observations (NSE was −134.8 and −71.4, respectively).

We additionally tested several modifications of these setups. These modifications included widening of the lateral structures (litter layer, lateral pathway, soil-bedrock interface) to two or three rows (corresponding to 0.10 and 0.15 m, respectively), increasing the density of vertical structures to an average separation of 0.5 m, limiting the vertical structures to the upper or lower half of the hillslope, varying the hydraulic conductivity of the macroporous structures (to $5 \times 10^{-2}\,\mathrm{m\,s^{-1}}$ and $5 \times 10^{-4}\,\mathrm{m\,s^{-1}}$, respectively), and increasing the hydraulic conductivity of the litter layer to the value assigned to the other structures, i.e., from $1.5 \times 10^{-4}\,\mathrm{m\,s^{-1}}$ to $5 \times 10^{-3}\,\mathrm{m\,s^{-1}}$. None of these modifications, however, did improve the results of the water flow simulation in terms of the selection criteria.

3.2 Observed and simulated solute dynamics

Transport of solute through the subsurface was simulated in 51 of the 65 basic setups, and 24 of these also fulfilled the surface runoff criterion. In these cases, the bulk of the simulated solute transport occurred via the implemented preferential pathways. No

solute transport in the subsurface was simulated with setups that either contained no structures, vertical structures without any lateral structures, or the soil-bedrock interface and/or the lateral pathway without any vertical structures.

The first breakthrough of tracer in the experiments at 28.7 m distance along the slope line was recorded after only 0.77 h, and the peak concentration was reached after 2.00 h (Wienhöfer et al., 2009a). The simulated solute transport was fast in some cases, but in no case as fast as in the observations. The solute transport simulations of the five runs found acceptable for water flow simulation (Fig. 4) yielded breakthrough times between 6.33 h and 6.92 h, and peak times between 8.25 h and 8.5 h, respectively (Table 4). The solute transport simulations of the remaining setups, including the tested modifications, essentially produced similar results.

In the experiment, only a small fraction of 13 % of the mobile tracer mass was recovered by the end of the first experimental stage considered in this paper (see Sect. 2.1.2). Recovery was much higher for the majority of the simulations (cf. Table 4). Consequently, the simulated and observed concentrations differed considerably. The observed maximum concentration in the outflow was 30.55 $\mu g L^{-1}$, which corresponds to a maximum transport rate of 3.12 $\mu g s^{-1}$. The highest maximum concentration in the simulations was 1406.76 $\mu g L^{-1}$, and the corresponding maximum transport rate was 170.38 $\mu g s^{-1}$ ("run109", Fig. 4). Only setups that contained a soil-bedrock interface and no additional lateral pathway had a recovery rate of less than 20 % due to increased storage of solute within the soil matrix ("run120", Table 4 and Fig. 4).

Because of these discrepancies in timing and magnitude of observed and simulated solute transport, the NSE criterion is not applicable. In order to compare the shapes of the observed and simulated breakthrough curves, we therefore calculated the maximum cross-correlation between the observed and simulated curves, which involved shifting the simulated curves in time to match the peak of the observations. The majority of the simulations showed good accordance with the shape of the observed breakthrough curve. Of the five acceptable setups, four yielded a maximum cross-correlation coefficient of 0.85 or higher (Table 4).

Title Page

Abstract | Introduction

Conclusions | References

Tables | Figures

◀ | ▶

◀ | ▶

Back | Close

Full Screen / Esc

Printer-friendly Version

Interactive Discussion

4 Discussion

The main objective of this study was to explore the modelling approach of representing preferential flow paths as distinct, connected elements in a 2-D numerical model.

We made use of the numerical model Catflow, which had also been used by Klaus and Zehe (2010, 2011) for modelling a tile-drained field site with explicit representation of earthworm burrows. The present paper expands on these studies by refining the approach and testing it on a different setting. Our study site is a steep forested hillslope, which is characterised by a shallow soil cover and macropores in form of pipes and desiccation cracks (Wienhöfer et al., 2009a). Accordingly, these structures were conceptualised being less tortuous and distributed more regularly over the hillslope, and we used a variable spatial resolution of the model with 0.05 m for the preferential flow paths and their surroundings, which appears more realistic compared to the constant resolution of 0.3 m used by Klaus and Zehe (2010). Further differences are that we assigned a uniform set of soil hydraulic parameters to each of the different soil types, without any random components, and that we did not apply any scaling of the width of the model domain to match the peak heights of the hydrographs. Similar to the Klaus and Zehe studies, the modelling approach allowed successful simulations of water flows at the hillslope scale. In contrast, the observed solute dynamics was not completely matched in the present study. In the following we flesh out and expand on these aspects through an examination of the specific experiences made with the simulation of water flows and solute transport in this work, and a general evaluation of advantages and limitations of the modelling approach with reference to the literature.

4.1 Simulation of preferential flow and hydrodynamic hillslope response

The modelling approach of representing preferential flow paths as distinct, connected elements of low flow resistivity was successful in several aspects. The approach allowed modelling the dominant processes of preferential infiltration into vertically oriented flow paths and subsequent preferential flow in laterally oriented structures, and

the outflow hydrograph of the hillslope was matched satisfactorily. Especially well fitted were the height and the onset of the outflow in response to sprinkling, and the magnitude and timing of the major peaks in response to natural rainfall, although the models were not calibrated on peak heights or in any other way. It is particularly remarkable that setups which matched the observed response to the steady-state rainfall simulation on parts of the hillslope also matched the observed response to natural rainfall on the entire surface area (Fig. 1), because only the hillslope width was used for scaling the input in between the two phases of the simulations. This fact suggests a certain predictive capability of these setups in conjunction with the modelling approach.

Flow in the distinct, finely-resolved preferential flow paths was the major component of the simulated hillslope outflow in the case of acceptable model setups. The observed hillslope hydrograph could not be reproduced with setups without any structures, and thus with a spatially constant soil parameterisation, even if a much higher hydraulic conductivity used. Surface runoff was the major component when the low hydraulic conductivity of the soil matrix was assigned to the entire soil material, while the outflow from the hillslope body was much more damped compared to the observations when higher hydraulic conductivities were used. Setups with only one type of structures similarly produced mainly surface runoff, and thus a more flashy response in comparison to the observations.

These findings show that a proper representation of the topology of the preferential flow network is the key to explain and reproduce the observed hydrological behaviour of the hillslope. This corroborates our perceptual model which had been based on plot-scale observations of preferential flow paths at the field site. More precisely, both lateral and vertical structures were needed for acceptable model runs, regardless of which density we modelled the vertical flow paths with or at which of the two depths the lateral flow path was positioned. The litter layer and the variable bedrock topography were not as important in the model. Other processes, as for example flow in the unsaturated soil matrix due to capillary forces and evapotranspiration, were of secondary importance

during the limited duration of the experiment, but were simulated in the model and would become significant during long-term simulations.

Of course, there was no complete and perfect match of simulated and observed hillslope outflow. The simulations differed from the observations during the recession phases, the peak heights of the three major peaks during natural rainfall were not matched equally well, and the small peak after the first major peak was not modelled by any of the simulations (Fig. 3). Although these deviations from the observed hillslope outflow may appear rather small in light of the fact that we are modelling the complex system of natural hillslope with a high degree of heterogeneity and a perfect fit of the model would never had been expected, it is illustrative to discuss this topic in further detail. Possible reasons for the mismatch of simulated and observed hillslope outflow could be up to the modelling approach in general or up to the specific implementation of the approach in this particular study. Another possible explanation would be incorrect observations, which cannot be fully excluded during field experiments. To simplify matters, we assume that the observations reported by Wienhöfer et al. (2009a) depict the hillslope hydrology correctly within typical ranges of uncertainty, and that these are reflected in the chosen acceptance criteria. Limitations of the modelling approach are related to the conceptualisation of preferential flow paths as highly porous media and the process representation using the Darcy–Richards equation, as well as to the reduction of the three-dimensional hillslope to a two-dimensional cross-section. These aspects are discussed in further detail in a following section. But even if conceptualisation and process description were perfect, the imperfect knowledge about the system itself would still lead to considerable uncertainty in setting up and parameterising a spatially explicit process model. The general lack of complete information on the internal build-up of a hydrological system basically makes it a "black box" for the modeller. This black box might be lightened up at selected "grey spots" where field observations for constraining the model setup are available, and has to be described by assumptions otherwise.

Predicting subsurface storm flow response

J. Wienhöfer and E. Zehe

Title Page

Abstract | Introduction

Conclusions | References

Tables | Figures

|◄ | ►|

◄ | ►

Back | Close

Full Screen / Esc

Printer-friendly Version

Interactive Discussion

This modelling study as well was based on assumptions in several aspects for which hard information was lacking. These assumptions could be replaced if site-specific data was available, which possibly, but not necessarily, might further improve the simulated hillslope response. For example, the assumption of spatially uniform rainfall input and canopy interception could be revisited, even if the influence of spatially variable throughfall on subsurface flow processes should only be secondary (Hopp and McDonnell, 2011; Bachmair and Weiler, 2012). Spatial variability of soil parameters was likewise unknown and not accounted for in the model setups; heterogeneity was represented solely by the different types of structures. Measured soul hydraulic parameters were only at hand for the fine-grained soil matrix from a single location, whereas soil hydraulic parameters for preferential flow structures, bedrock and litter layer have been chosen arbitrarily or from the literature. Variations of the hydraulic conductivity values, however, did not yield better-fitting parameter combinations. Finally, the unknown subsurface flow paths were modelled with a random component, but in a rather regular basic arrangement for better comparability. It cannot be ruled that other, perhaps more irregular patterns would deliver comparable or better results. The tested modifications, for example limiting vertical flow paths to the upper or the lower half of the hillslope, did not improve the results.

4.2 Simulation of preferential flow and solute transport

In contrast to the successful water flow simulations, the solute transport simulations yielded ambivalent results. The modelling approach allowed simulating solute transport via the preferential flow paths, and spread and shape of the observed breakthrough curve were matched well by several simulations, which corroborates that adequate modelling of macroscopic dispersion is a by-product of the explicit consideration of distinctive structures as shown by Vogel et al. (2006). In order to allow simulation of solute transport in the spatially explicit flow paths, however, a slight modification of the numerical tool Catflow was required. We found during preliminary tests that the internal interpolation of flow velocities for the random walk particle tracking led to a trapping

J. Wienhöfer and E. Zehe

of particles adjacent to the implemented structures. This phenomenon has been described earlier (LaBolle et al., 1996), and is particular serious in the case of finely resolved materials with highly contrasting properties as in our study. Turning off the interpolation of local flow velocities for the particle step kept the velocities contrasts between matrix and structures, and avoided the trapping of solute in the soil matrix. The change in the code only affected the simulation of solute transport and not the water flow calculation. Still, none of the simulations captured the very fast breakthrough and early peak of the tracer. In principle, a similar reasoning as for the water flow simulation would apply for explaining minor discrepancies in the solute transport simulation, which could for instance result from the specific parameterisation or arrangement of structures. The systematic mismatch in transport velocities, however, points to another fundamental problem based in the modelling concept.

The solute is modelled as a conservative tracer with low molecular diffusivity, and solute transport is thus closely related to the water flow simulation. The simulated breakthrough curve and accordingly the flow velocity distribution indeed matched spread and shape of the observed breakthrough curve, but its location was heavily shifted and the effective flow velocities were systematically underestimated. This can be explained by the fact that matching of the hydrographs only requires a good estimate of the vertical and lateral water flux densities or filter velocities, which control the total water flow through a model cross section. Advective solute transport is, however, controlled by pore velocities defined as the ratio of the filter velocity and the active cross-section where transport takes place, which is much smaller than the product of porosity and the cross-sectional area of the flow domain in case of preferential flow. The hillslope was modelled spatially explicit and finely resolved in the vertical and downslope direction, but is assumed homogeneous perpendicular to the slope line in the two-dimensional model. This implies that the distinctive structures extended over the entire width of the hillslope in this direction. Admittedly, this is unrealistic assumption, which implies artificially reduced pore water velocities and thus advective transport velocities.

Filter velocities were modelled in an acceptable manner, as demonstrated by the successful match of the hydraulic response achieved with the behavioural model setups, and thus higher transport velocities would be obtained by reducing the cross-sectional area in which flow and transport take place. Observed and simulated peak velocity differed approximately by factor four in the successful setups, indicating a reduction of the fraction of distinctive structures to 25 % or less of the width of the hillslope would lead to fitting flow velocities in the model. Interestingly, this value roughly corresponds to the areal fraction of preferential flow paths of about 20 % found with dye staining experiments at the plot scale (Wienhöfer et al., 2009a). Higher transport velocities could be achieved within a 2-D model by introducing an areal fraction of macropores as suggested by Zehe and Blöschl (2004). But use of a particle tracking approach would additionally require the implementation of a reflection principle (LaBolle et al., 1996) to prevent unintentional overshoot of solute particles out of the structures. The best solution in line with the idea of considering structures explicitly, however, would be to change over to 3-D simulation tools and test their capabilities for solute transport simulation in connection with finely resolved distinctive flow paths.

Another peculiarity of the tracer observations was the low recovery rate, which was only partly due to the irreversible sorption within the top soil (Wienhöfer et al., 2009a). While most of the simulations with solute transport resulted in high recovery rates, a low recovery was found with setups which featured vertical structures and a soil-bedrock interface, but no lateral pathway (e.g., "run120", Tables 3 and 4). A lower recovery rate could possibly be considered an additional criterion for selecting these setups, if also the timing and shape of the simulated breakthrough curves were closer to the observations.

4.3 Advantages and limitations of the modelling approach

In our model, water flows are simulated using Richards' equation, and preferential flow pathways are conceptualised as an artificial porous medium with low flow resistivity and low retention capability. With application of this concept, we accept the trade-off

between the possibility to incorporate preferential flow in distinctive structures into an existing numerical model, and possible errors resulting from the use of Richards' equation for water flows in these structure, which would rigorously have to be deemed inappropriate for describing flow and frictional losses in macropores (Beven and Germann, 1982). Despite this inconsistency, the concept has been proposed for representing macropore flow in single-domain (Nieber and Warner, 1991) and dual-domain (Gerke and Vangenuchten, 1993) soil hydrological models. Especially with spatially explicit single-domain models, the implementation of distinctive structures is straightforward by choosing a respective parameterisation for corresponding model regions as done in the present study, and this approach was successfully applied in modeling controlled experiments at the lab-scale (Castiglione et al., 2003; Lamy et al., 2009) and the plot-scale (Vogel et al., 2006; Nieber and Sidle, 2010). From this research it was concluded that exact flow rules are not the only concern (Lamy et al., 2009), and successful modelling of preferential flow is possible even with an approximate flow law such as the Richards' equation if at the same time an approximate representation of structures is taken into account (Vogel et al., 2006).

In our application of the approach at the hillslope scale, the exact configuration of the complete preferential flow network was unknown, and we used a hypothetical network of vertical and lateral flow paths of limited spatial extent to conceptualise the structural heterogeneity of the hillslope observed at the plot-scale. These flow paths are not supposed to represent single structures spanning the entire hillslope, or structures of a single origin, but we rather hypothesise a network of connected flow paths constituted by several individual macropores, such as root holes, desiccation cracks and animal burrows, which are either connected directly to each other or via zones of higher porosity sustained by biological and/or hydrological processes When these pathways are modelled as a highly porous medium, we implicitly include the surrounding matrix that might as well contribute to preferential flow (Lamy et al., 2009). Functional connectivity of individual macropores controlled by saturation state is implicitly modelled as well, as dry portions of the flow network will act as flow barriers in the simulation.

Several different combinations of vertical and lateral pathways were equally successful in simulating the hillslope. This equifinality in structural setups was also reported in earlier studies (Weiler and McDonnell, 2007; Klaus and Zehe, 2010, 2011). Additional field evidence would be needed to better constrain the structural patterns a priori, or to narrow the selection from successful combinations of structures. Klaus and Zehe (2011) were able to reduce the number of acceptable setups by evaluating the capability to simulate tracer transport. This was not possible in this study, given the very similar results of tracer transport simulations. The presence of structural equifinality is not necessarily a drawback of the concept, since it implies that the exact configuration of subsurface flow paths does not need to be known explicitly to simulate lateral preferential subsurface flow at the hillslope scale (Weiler and McDonnell, 2007).

Our results suggest a dominant role of vertical and lateral flow paths for the hydrological response at the hillslope scale. This is in line with findings from earlier modelling studies that considered flow in distinctive structures in their models (Sidle et al., 2001; Jones and Connelly, 2002; Weiler and McDonnell, 2007). The role of variable bedrock topography, however, was subordinate in our model, which is in contrast to the findings of modelling studies without explicit consideration of structures (Weiler and McDonnell, 2004; Hopp and McDonnell, 2009; James et al., 2010). For example, Stadler et al. (2012) employed a 2-D dual-permeability model for the same site, and successfully simulated the hydraulic response to the first phase of the sprinkling experiment. They also found that flow predominantly occurred in the macropore domain, but as this was modelled spatially constant and isotropic within the soil mantle, the variable bedrock surface – the same as used in this study – exerted much more control on lateral preferential flows than in our model, in which lateral pathways were present. This is an illustrative example for the basic fact that possible model outcomes are generally bound to the inherent assumptions of the underlying perceptual and conceptual models. Another issue is the simplification of the hillslope as a vertical 2-D cross-section. The reduction to 2-D tends to underestimate connectivity compared to a 3-D realisation when treating heterogeneous porous media as a random field (Fiori and Jankovic,

Predicting subsurface storm flow response

J. Wienhöfer and E. Zehe

Title Page

Abstract | Introduction

Conclusions | References

Tables | Figures

◀ | ▶

◀ | ▶

Back | Close

Full Screen / Esc

Printer-friendly Version

Interactive Discussion

2012). In our study this was far less a problem, as preferential flow paths were modelled explicitly and connectivity was hence prescribed a priori. The topology of the flow network was represented sufficiently for the simulation of hydraulic response in a 2-D model, not least because the study hillslope was much longer than its width, and the line of steepest descent in potential energy serves as symmetry axis. The simplification to 2-D, however, restricted the explicit representation of distinctive structures in the third dimension, which caused the mismatch in solute transport discussed above. Future studies should thus consider the use of 3-D models, if solute transport in distinctive structures is to be simulated. The concept of explicit representation of structures could possibly be implemented in a similar way into 3-D models that found recent attention for performing virtual experiments at the hillslope scale (Hopp and McDonnell, 2009; James et al., 2010), but this remains subject of further research.

5 Conclusions

This paper implements and evaluates the concept of incorporating preferential flow paths explicitly as distinctive structures in a process-based model. The approach was applied within the 2-D numerical model Catflow for modelling water flows and solute transport observed during a field experiment at a steep forested hillslope. The model successfully represented hillslope hydrological response by depicting the sharp contrast in flux density between structures and matrix, and the configurations of successful model setups suggest that preferential flow bound to structures is a first-order control on the hydrology of the study hillslope, whereas spatial variability of soil depth is secondary. The solute transport simulations with these setups matched spread and shape of the observed breakthrough curve well, indicating that macrodispersion induced by preferential flow was captured well by the topology of the preferential flow network, but the model could not match the fast breakthrough times observed in the tracer experiment. This can readily be attributed to the incorrect representation of the spatial dimensions of the implemented distinctive structures in the 2-D cross-section, which

Predicting subsurface storm flow response

J. Wienhöfer and E. Zehe

leaded to an underestimation of effective transport velocities in comparison with correctly modelled flux densities.

We employed an established numerical model as a virtual reality in the sense that we model the unknown instead of searching for a suitable process description in a completely controlled system. The results of this study show that not only the flow equations and the numerical implementation have to fit the processes to be modelled, and that this has to be checked critically, but that also perception and conceptualisation of the system play a decisive role in the modelling process. Possible model outcomes are always bound to the assumptions inherent in the underlying perceptual and conceptual models and limitations of the numerical tool, and it is therefore mandatory to use a model with adequate complexity to include a wide range of possible processes. Because of their possibly dominating role, distinctive structures should thus be included in models used as virtual experiments to advance the understanding of hillslope controls on hydrological processes such as subsurface stormflow.

Title Page

Abstract | Introduction

Conclusions | References

Tables | Figures

◀ | ▶

◀ | ▶

Back | Close

Full Screen / Esc

Printer-friendly Version

Interactive Discussion

References

Abou Najm, M. R., Jabro, J. D., Iversen, W. M., Mohtar, R. H., and Evans, R. G.: New method for the characterization of three-dimensional preferential flow paths in the field, Water Resour. Res., 46, W02503, doi:10.1029/2009wr008594, 2010.

Allaire, S. E., Gupta, S. C., Nieber, J., and Moncrief, J. F.: Role of macropore continuity and tortuosity on solute transport in soils: 1. Effects of initial and boundary conditions, J. Contam. Hydrol., 58, 299–321, doi:10.1016/s0169-7722(02)00035-9, 2002a.

Allaire, S. E., Gupta, S. C., Nieber, J., and Moncrief, J. F.: Role of macropore continuity and tortuosity on solute transport in soils: 2. Interactions with model assumptions for macropore description, J. Contam. Hydrol., 58, 283–298, doi:10.1016/s0169-7722(02)00034-7, 2002b.

Anderson, A. E., Weiler, M., Alila, Y., and Hudson, R. O.: Subsurface flow velocities in a hillslope with lateral preferential flow, Water Resour. Res., 45, W11407, doi:10.1029/2008wr007121, 2009a.

Anderson, A. E., Weiler, M., Alila, Y., and Hudson, R. O.: Dye staining and excavation of a lateral preferential flow network, Hydrol. Earth Syst. Sci., 13, 935–944, doi:10.5194/hess-13-935-2009, 2009b.

Bachmair, S. and Weiler, M.: Hillslope characteristics as controls of subsurface flow variability, Hydrol. Earth Syst. Sci., 16, 3699–3715, doi:10.5194/hess-16-3699-2012, 2012.

Baram, S., Kurtzman, D., and Dahan, O.: Water percolation through a clayey vadose zone, J. Hydrol., 424, 165–171, doi:10.1016/j.jhydrol.2011.12.040, 2012.

Beven, K. and Germann, P.: Macropores and water-flow in soils, Water Resour. Res., 18, 1311–1325, 1982.

Bievre, G., Jongmans, D., Winiarski, T., and Zumbo, V.: Application of geophysical measurements for assessing the role of fissures in water infiltration within a clay landslide (Trieves area, French Alps), Hydrol. Process., 26, 2128–2142, doi:10.1002/hyp.7986, 2012.

Buttle, J. M. and McDonald, D. J.: Coupled vertical and lateral preferential flow on a forested slope, Water Resour. Res., 38, 18.11–18.16, doi:10.1029/2001wr000773, 2002.

Casalini, T., Salvalaglio, M., Perale, G., Masi, M., and Cavallotti, C.: Diffusion and aggregation of sodium fluorescein in aqueous solutions, J. Phys. Chem. B, 115, 12896–12904, doi:10.1021/jp207459k, 2011.

Title Page

Abstract | Introduction

Conclusions | References

Tables | Figures

◀ | ▶

◀ | ▶

Back | Close

Full Screen / Esc

Printer-friendly Version

Interactive Discussion

Castiglione, P., Mohanty, B. P., Shouse, P. J., Simunek, J., van Genuchten, M. T., and Santini, A.: Lateral water diffusion in an artificial macroporous system, Vadose Zone J., 2, 212–221, 2003.

Celia, M. A., Bouloutas, E. T., and Zarba, R. L.: A general mass-conservative numerical-solution for the unsaturated flow equation, Water Resour. Res., 26, 1483–1496, doi:10.1029/90wr00196, 1990.

Durner, W.: Hydraulic conductivity estimation for soils with heterogeneous pore structure, Water Resour. Res., 30, 211–223, 1994.

Fiori, A. and Jankovic, I.: On preferential flow, channeling and connectivity in heterogeneous porous formations, Math. Geosci., 44, 133–145, doi:10.1007/s11004-011-9365-2, 2012.

Flury, M., Flühler, H., Jury, W. A., and Leuenberger, J.: Susceptibility of soils to preferential flow of water – a field-study, Water Resour. Res., 30, 1945–1954, 1994.

Gerke, H. H.: Preferential flow descriptions for structured soils, J. Plant Nutr. Soil Sc., 169, 382–400, doi:10.1002/jpln.200521955, 2006.

Gerke, H. H. and Vangenuchten, M. T.: A dual-porosity model for simulating the preferential movement of water and solutes in structured porous-media, Water Resour. Res., 29, 305–319, 1993.

Graeff, T., Zehe, E., Reusser, D., Lueck, E., Schroeder, B., Wenk, G., John, H., and Bronstert, A.: Process identification through rejection of model structures in a mid-mountainous rural catchment: observations of rainfall-runoff response, geophysical conditions and model inter-comparison, Hydrol. Process., 23, 702–718, doi:10.1002/hyp.7171, 2009.

Greve, A. K., Acworth, R. I., and Kelly, B. F. J.: Detection of subsurface soil cracks by vertical anisotropy profiles of apparent electrical resistivity, Geophysics, 75, WA85–WA93, doi:10.1190/1.3474590, 2010.

Hopp, L. and McDonnell, J. J.: Connectivity at the hillslope scale: identifying interactions between storm size, bedrock permeability, slope angle and soil depth, J. Hydrol., 376, 378–391, doi:10.1016/j.jhydrol.2009.07.047, 2009.

Hopp, L. and McDonnell, J. J.: Examining the role of throughfall patterns on subsurface stormflow generation, J. Hydrol., 409, 460–471, doi:10.1016/j.jhydrol.2011.08.044, 2011.

James, A. L., McDonnell, J. J., Tromp-Van Meerveld, I., and Peters, N. E.: Gypsies in the palace: experimentalist's view on the use of 3-D physics-based simulation of hillslope hydrological response, Hydrol. Process., 24, 3878–3893, 2010.

Title Page

Abstract | Introduction

Conclusions | References

Tables | Figures

◄ | ►

◄ | ►

Back | Close

Full Screen / Esc

Printer-friendly Version

Interactive Discussion

Jarvis, N. J.: A review of non-equilibrium water flow and solute transport in soil macropores: principles, controlling factors and consequences for water quality, Eur. J. Soil Sci., 58, 523–546, 2007.

Jones, J. A. A. and Connelly, L. J.: A semi-distributed simulation model for natural pipeflow, J. Hydrol., 262, 28–49, 2002.

Kelln, C. J., Barbour, S. L., and Qualizza, C.: Fracture-dominated subsurface flow and transport in a sloping reclamation cover, Vadose Zone J., 8, 96–107, doi:10.2136/vzj2008.0064, 2009.

Kienzler, P. M. and Naef, F.: Subsurface storm flow formation at different hillslopes and implications for the "old water paradox", Hydrol. Process., 22, 104–116, 2008.

Klaus, J. and Zehe, E.: Modelling rapid flow response of a tile-drained field site using a 2-D physically based model: assessment of "equifinal" model setups, Hydrol. Process., 24, 1595–1609, doi:10.1002/hyp.7687, 2010.

Klaus, J. and Zehe, E.: A novel explicit approach to model bromide and pesticide transport in connected soil structures, Hydrol. Earth Syst. Sci., 15, 2127–2144, doi:10.5194/hess-15-2127-2011, 2011.

Köhne, J. M., Köhne, S., and Šimůnek, J.: A review of model applications for structured soils: a) water flow and tracer transport, J. Contam. Hydrol., 104, 4–35, doi:10.1016/j.jconhyd.2008.10.002, 2009.

Kosugi, K., Uchida, T., and Mizuyama, T.: Numerical calculation of soil pipe flow and its effect on water dynamics in a slope, Hydrol. Process., 18, 777–789, 2004.

LaBolle, E. M., Fogg, G. E., and Tompson, A. F. B.: Random-walk simulation of transport in heterogeneous porous media: local mass-conservation problem and implementation methods, Water Resour. Res., 32, 583–593, doi:10.1029/95wr03528, 1996.

Lamy, E., Lassabatere, L., Bechet, B., and Andrieu, H.: Modeling the influence of an artificial macropore in sandy columns on flow and solute transfer, J. Hydrol., 376, 392–402, doi:10.1016/j.jhydrol.2009.07.048, 2009.

Lindenmaier, F.: Hydrology of a Large Unstable Hillslope at Ebnit, Vorarlberg – Identifying Dominating Processes and Structures, Ph.D. thesis, Institute of Geoecology, University of Potsdam, Potsdam, Germany, 154 pp., 2008.

Lindenmaier, F., Zehe, E., Dittfurth, A., and Ihringer, J.: Process identification at a slow-moving landslide in the Vorarlberg Alps, Hydrol. Process., 19, 1635–1651, 2005.

Title Page

Abstract | Introduction

Conclusions | References

Tables | Figures

◀ | ▶

◀ | ▶

Back | Close

Full Screen / Esc

Printer-friendly Version

Interactive Discussion

Luxmoore, R. J., Jardine, P. M., Wilson, G. V., Jones, J. R., and Zelazny, L. W.: Physical and chemical controls of preferred path flow through a forested hillslope, Geoderma, 46, 139–154, 1990.

Maurer, T.: Physikalisch begründete, zeitkontinuierliche Modellierung des Wassertransports in kleinen ländlichen Einzugsgebieten, Ph.D. thesis, Fakultät für Bauingenieur- und Vermessungswesen, Universität Karlsruhe (TH), Karlsruhe, Germany, 224 pp., 1997.

McDonnell, J. J., Sivapalan, M., Vaché, K., Dunn, S., Grant, G., Haggerty, R., Hinz, C., Hooper, R., Kirchner, J., Roderick, M. L., Selker, J., and Weiler, M.: Moving beyond heterogeneity and process complexity: a new vision for watershed hydrology, Water Resour. Res., 43, W07301, doi:10.1029/2006wr005467, 2007.

Moysey, S. M. J. and Liu, Z.: Can the onset of macropore flow be detected using electrical resistivity measurements?, Soil Sci. Soc. Am. J., 76, 10–17, doi:10.2136/sssaj2010.0413, 2012.

Mualem, Y.: A new model for predicting the hydraulic conductivity of unsaturated porous media, Water Resour. Res., 12, 513–522, doi:10.1029/WR012i003p00513, 1976.

Nieber, J. L. and Sidle, R. C.: How do disconnected macropores in sloping soils facilitate preferential flow?, Hydrol. Process., 24, 1582–1594, doi:10.1002/Hyp.7633, 2010.

Nieber, J. L. and Warner, G. S.: Soil pipe contribution to steady subsurface stormflow, Hydrol. Process., 5, 329–344, doi:10.1002/hyp.3360050402, 1991.

Noguchi, S., Tsuboyama, Y., Sidle, R. C., and Hosoda, I.: Morphological characteristics of macropores and the distribution of preferential flow pathways in a forested slope segment, Soil Sci. Soc. Am. J., 63, 1413–1423, 1999.

Peters, D. L., Buttle, J. M., Taylor, C. H., and Lazerte, B. D.: Runoff production in a forested, shallow soil, Canadian Shield Basin, Water Resour. Res., 31, 1291–1304, 1995.

R Development Core Team: R: A Language and Environment for Statistical Computing, R Foundation for Statistical Computing, Vienna, Austria, available at: http://www.R-project.org (last access: 13 May 2013), 2011.

Roth, K. and Hammel, K.: Transport of conservative chemical through an unsaturated two-dimensional Miller-similar medium with steady state flow, Water Resour. Res., 32, 1653–1663, doi:10.1029/96wr00756, 1996.

Samouelian, A., Cousin, I., Richard, G., Tabbagh, A., and Bruand, A.: Electrical resistivity imaging for detecting soil cracking at the centimetric scale, Soil Sci. Soc. Am. J., 67, 1319–1326, 2003.

Predicting subsurface storm flow response

J. Wienhöfer and E. Zehe

Title Page

| Abstract | Introduction |

| Conclusions | References |

| Tables | Figures |

◄ | ►|

◄ | ►

Back | Close

Full Screen / Esc

Printer-friendly Version

Interactive Discussion

Sanders, E. C., Abou Najm, M. R., Mohtar, R. H., Kladivko, E., and Schulze, D.: Field method for separating the contribution of surface-connected preferential flow pathways from flow through the soil matrix, Water Resour. Res., 48, W04534, doi:10.1029/2011wr011103, 2012.

Schulz, K., Seppelt, R., Zehe, E., Vogel, H. J., and Attinger, S.: Importance of spatial structures in advancing hydrological sciences, Water Resour. Res., 42, W03S03, doi:10.1029/2005wr004301, 2006.

Sidle, R. C., Noguchi, S., Tsuboyama, Y., and Laursen, K.: A conceptual model of preferential flow systems in forested hillslopes: evidence of self-organization, Hydrol. Process., 15, 1675–1692, 2001.

Šimůnek, J., Jarvis, N. J., van Genuchten, M. T., and Gardenas, A.: Review and comparison of models for describing non-equilibrium and preferential flow and transport in the vadose zone, J. Hydrol., 272, 14–35, 2003.

Sobieraj, J. A., Elsenbeer, H., and Cameron, G.: Scale dependency in spatial patterns of saturated hydraulic conductivity, Catena, 55, 49–77, 2004.

Stadler, L., Hinkelmann, R., and Helmig, R.: Modeling macroporous soils with a two-phase dual-permeability model, Transport Porous Med., 95, 585–601, doi:10.1007/s11242-012-0064-3, 2012.

Tabbagh, J., Samouëlian, A., Tabbagh, A., and Cousin, I.: Numerical modelling of direct current electrical resistivity for the characterisation of cracks in soils, J. Appl. Geophys., 62, 313–323, doi:10.1016/j.jappgeo.2007.01.004, 2007.

Tsutsumi, D., Sidle, R. C., and Kosugi, K.: Development of a simple lateral preferential flow model with steady state application in hillslope soils, Water Resour. Res., 41, W12420, doi:10.1029/2004wr003877, 2005.

Uchida, T., Tromp-van Meerveld, I., and McDonnell, J. J.: The role of lateral pipe flow in hillslope runoff response: an intercomparison of non-linear hillslope response, J. Hydrol., 311, 117–133, 2005.

Van Genuchten, M. T.: A closed-form equation for predicting the hydraulic conductivity of unsaturated soils, Soil Sci. Soc. Am. J., 44, 892–898, 1980.

Vogel, H. J. and Roth, K.: Moving through scales of flow and transport in soil, J. Hydrol., 272, 95–106, 2003.

Vogel, H.-J., Cousin, I., Ippisch, O., and Bastian, P.: The dominant role of structure for solute transport in soil: experimental evidence and modelling of structure and transport in a field experiment, Hydrol. Earth Syst. Sci., 10, 495–506, doi:10.5194/hess-10-495-2006, 2006.

Title Page

Abstract | Introduction

Conclusions | References

Tables | Figures

|◄ | ►|

◄ | ►

Back | Close

Full Screen / Esc

Printer-friendly Version

Interactive Discussion

Weiler, M. and McDonnell, J.: Virtual experiments: a new approach for improving process conceptualization in hillslope hydrology, J. Hydrol., 285, 3–18, 2004.

Weiler, M. and McDonnell, J. J.: Conceptualizing lateral preferential flow and flow networks and simulating the effects on gauged and ungauged hillslopes, Water Resour. Res., 43, W03403, doi:10.1029/2006WR004867, 2007.

Wienhöfer, J., Germer, K., Lindenmaier, F., Färber, A., and Zehe, E.: Applied tracers for the observation of subsurface stormflow at the hillslope scale, Hydrol. Earth Syst. Sci., 13, 1145–1161, doi:10.5194/hess-13-1145-2009, 2009a.

Wienhöfer, J., Lindenmaier, F., Ihringer, J., and Zehe, E.: Characterization of soil hydraulic properties on a creeping alpine slope, in: Hydrology in Mountain Regions: Observations, Processes and Dynamics, edited by: Marks, D., IAHS Publication, 326, IAHS Press, Wallingford, UK, 3–10, 2009b.

Wienhöfer, J., Lindenmaier, F., and Zehe, E.: Challenges in understanding the hydrologic controls on the mobility of slow-moving landslides, Vadose Zone J., 10, 496–511, doi:10.2136/vzj2009.0182, 2011.

Zehe, E. and Blöschl, G.: Predictability of hydrologic response at the plot and catchment scales: role of initial conditions, Water Resour. Res., 40, W10202, doi:10.1029/2003wr002869, 2004.

Zehe, E. and Flühler, H.: Preferential transport of isoproturon at a plot scale and a field scale tile-drained site, J. Hydrol., 247, 100–115, 2001.

Zehe, E., Maurer, T., Ihringer, J., and Plate, E.: Modeling water flow and mass transport in a loess catchment, Phys. Chem. Earth Pt. B, 26, 487–507, doi:10.1016/s1464-1909(01)00041-7, 2001.

Zehe, E., Becker, R., Bardossy, A., and Plate, E.: Uncertainty of simulated catchment runoff response in the presence of threshold processes: role of initial soil moisture and precipitation, J. Hydrol., 315, 183–202, 2005.

Zehe, E., Blume, T., and Bloeschl, G.: The principle of "maximum energy dissipation": a novel thermodynamic perspective on rapid water flow in connected soil structures, Philos. T. Roy. Soc. B, 365, 1377–1386, doi:10.1098/rstb.2009.0308, 2010a.

Zehe, E., Graeff, T., Morgner, M., Bauer, A., and Bronstert, A.: Plot and field scale soil moisture dynamics and subsurface wetness control on runoff generation in a headwater in the Ore Mountains, Hydrol. Earth Syst. Sci., 14, 873–889, doi:10.5194/hess-14-873-2010, 2010b.

Title Page

Abstract | Introduction

Conclusions | References

Tables | Figures

|◄ | ►|

◄ | ►

Back | Close

Full Screen / Esc

Printer-friendly Version

Interactive Discussion

J. Wienhöfer and E. Zehe

Table 1. Overview on model setup variants: five different types of structures have been considered in different realisations for generating the structural setups. All 64 combinations of the "systematic model variants" have been tested for simulation, plus modifications of selected combinations given as "additional model variants".

Type of structure	Systematic model variants	Additional model variants
Litter layer	– thickness 2.5 cm – none	– thickness 7.5 cm – higher hydraulic conductivity $(2.5 \times 10^{-2}\,\mathrm{m\,s^{-1}})$
Vertical structures	– separation 1 m – separation 2 m – separation 4 m – none	– separation 0.5 m – limitation to upper or lower half of hillslope
Lateral structure	– thickness 5.0 cm – none	– thickness 10.0 cm – hydraulic conductivity set to 10 % $(5.0 \times 10^{-4}\,\mathrm{m\,s^{-1}})$ and 500 % $(2.5 \times 10^{-2}\,\mathrm{m\,s^{-1}})$
Soil-bedrock interface	– thickness 5.0 cm – none	– thickness 10.0 cm
Bedrock	– variable soil depth: steepest descent of kriged topography – constant soil depth: mean value of variable topography	– no bedrock

Table 2. Hydraulic and transport parameter values used for different materials in the model.

Type of structure	Saturated hydraulic conductivity K_s [m s^{-1}]	Total porosity Θ_s [–]	Residual water content Θ_r [–]	Reciprocal air entry value α [m^{-1}]	Shape parameter n [–]	Dispersion coefficient D [m^2 s^{-1}]
Litter layer	1.50×10^{-4}	0.60	0.05	0.50	1.70	1.00×10^{-8}
Vertical and lateral structures, soil-bedrock interface	5.00×10^{-3}	0.60	0.30	1.00	2.00	1.00×10^{-8}
Soil matrix	1.77×10^{-7}	0.55	0.11	0.08	1.09	1.00×10^{-6}
Bedrock	5.00×10^{-9}	0.35	0.11	0.50	2.00	1.00×10^{-9}

Full Screen / Esc

Printer-friendly Version

Interactive Discussion

J. Wienhöfer and E. Zehe

Title Page

Abstract   Introduction

Conclusions   References

Tables   Figures

◀◀   ▶▶

◀   ▶

Back   Close

Full Screen / Esc

Printer-friendly Version

Interactive Discussion

Table 3. Structural features of model setups selected as acceptable for the hydrograph simulations with a Nash–Sutcliffe efficiency (NSE) greater than 0.75, a water balance error less than 10 %, and surface runoff less than 10 % of total outflow during the sprinkling phase (surface runoff ratio); "+" indicates presence of the respective structural feature.

ID	Litter layer	Vertical structures (separation)	Lateral pathway	Soil-bedrock interface	Depth to bedrock	NSE	Water balance error [%]	Surface runoff ratio [%]
run107		+ (1 m)	+		constant	0.83	−3	5
run109		+ (1 m)	+	+	constant	0.76	−4	5
run111	+	+ (2 m)	+		constant	0.78	3	1
run119	+	+ (4 m)	+		constant	0.86	9	7
run120	+	+ (4 m)		+	constant	0.83	5	7

J. Wienhöfer and E. Zehe

Table 4. Summary of solute transport characteristics of simulations and observation: times to breakthrough and peak, recovery of tracer, maximum cross correlation of observed and simulated breakthrough curves, and ratio of simulated and observed peak velocities. The recovery of the observation is the value corrected for irreversible sorption in the top soil reported by Wienhöfer et al. (2009a).

ID	Time to breakthrough [h]	Time to peak [h]	Recovery [%]	Maximum cross correlation	Peak velocity ratio
run107	6.83	8.33	94.98	0.986	0.24
run109	6.92	8.50	95.27	0.986	0.24
run111	6.33	8.25	91.58	0.940	0.24
run119	6.58	8.42	89.61	0.864	0.24
run120	6.92	8.42	15.25	0.730	0.24
observed	0.77	2.00	13.32	–	–
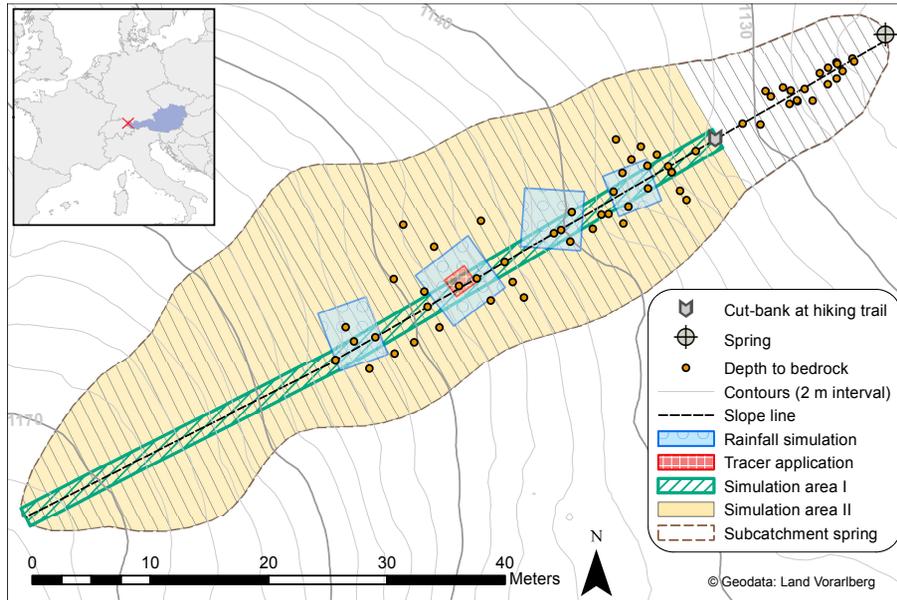
Fig. 1. Map of the study hillslope showing locations of field observations and experimental plots as well as simulation areas considered for model setup. The inlet shows the location of the study area within Europe.
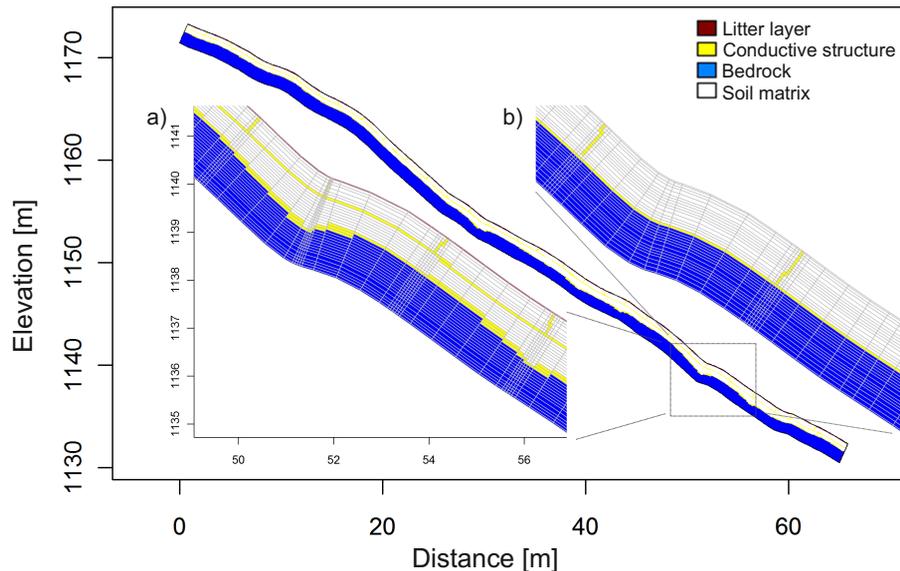
Fig. 2. Setup of hillslope model in profile view; the insets show enlarged detail with different realisations of explicit structures: **(a)** setup with litter layer, vertical flow paths (2 m spacing), lateral flow path, and soil-bedrock interface layer on interpolated bedrock topography. **(b)** setup with widely spaced vertical flow paths (4 m spacing) and soil-bedrock interface layer at constant soil depth over the entire profile; the inset is at the same scale as inset **(a)**.
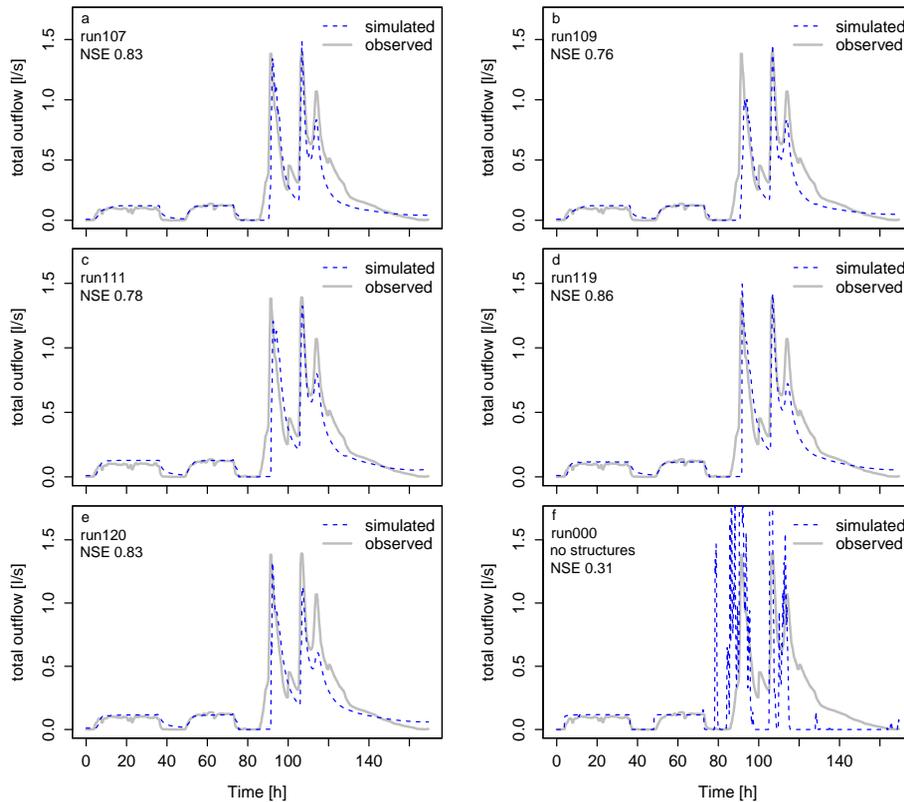
Fig. 3. Observed hydrographs and simulated total outflow of the five acceptable model setups **(a–e)** and of a setup without any structures **(f)**. The identifier and the Nash–Sutcliffe efficiency (NSE) are given in the upper left corner of each panel; time is given as hours since beginning of sprinkling experiment.

Title Page

Abstract | Introduction

Conclusions | References

Tables | Figures

|◄ | ►|

◄ | ►

Back | Close

Full Screen / Esc

Printer-friendly Version

Interactive Discussion
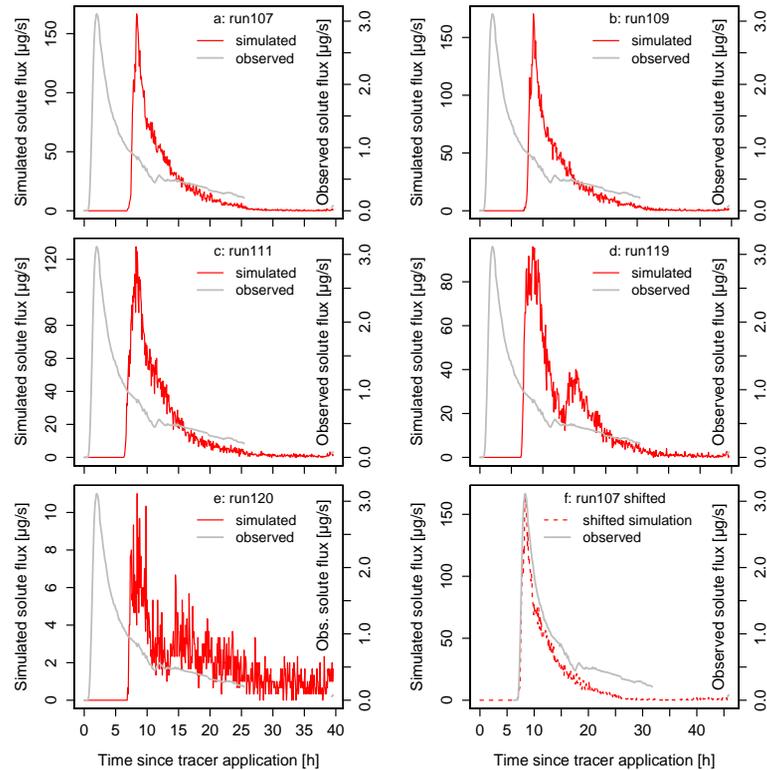
Fig. 4. Solute breakthrough curves of the five acceptable setups and the observation **(a–e)**, and comparison of the shape of observed and shifted simulated breakthrough curves, obtained by shifting the simulated peak to match peak of the observation **(f)**. Time is given as hours since tracer application.